Hindawi
Advances in Materials Science and Engineering
Volume 2023, Article ID 8275323, 10 pages
https://doi.org/10.1155/2023/8275323

Research Article

Optimization and Characterization Studies of Dissimilar Friction Stir Welding Parameters of Brass and Aluminum Alloy 6063 Using Taguchi

Vimal Agarwal,[1] Deepam Goyal,[2] B. S. Pabla,[1] S. C. Vettivel,[3] and A. Haiter Lenin [4]

[1]*Department of Mechanical Engineering, NITTTR, Chandigarh, India*
[2]*Chitkara University Institute of Engineering and Technology, Chitkara University, Chandigarh, Punjab, India*
[3]*Department of Mechanical Engineering, CCET (Degree Wing), Sector 26, Chandigarh, India*
[4]*Department of Mechanical Engineering, Wollo University, Kombolcha Institute of Technology, Post Box No: 208, Kombolcha, Ethiopia*

Correspondence should be addressed to A. Haiter Lenin; drahlenin@wu.edu.et

Received 19 July 2022; Revised 28 November 2022; Accepted 26 April 2023; Published 31 May 2023

Academic Editor: M. Adam Khan

This paper focuses on optimizing process parameters such as tool rotating speed, preheat-treated workpiece temperature, traverse speed, and tool pin profile for dissimilar friction stir welding (FSW) of brass and AA 6063. The hardness of the friction stir-welded joint created is measured as a response variable. The Taguchi design of experiments approach was utilized to finalize the experimental strategy, and ANOVA was employed to analyze the data. The best input factors for a better weld and a harder FSW workpiece were predicted. The experimental results show that the input factors influenced the hardness and defects in the welds in the following order: tool rotation speed (28.98%), tool pin geometry (22.30%), travel speed (11%), and temperature of the preheat treated workpiece (10.95%), respectively. Optical microscopy identified three distinct zones: the nugget zone, the thermo-mechanically affected zone, and the heat-affected zone. The nugget zone had a maximum value of hardness (around a 27% increase) due to the formation of very fine recrystallized grains.

1. Introduction

Aluminium alloys (AA) are used in an expanding range of engineering applications, such as the automotive and aerospace industries, because of their excellent machinability, high stress-to-weight ratios, and superb corrosion resistance. However, there are some problems during the joining of Al alloys using conventional fusion welding techniques because of high distortion, generation of secondary brittle phases, residual stresses, and cracking during solidification [1]. In 1991, Thomas et al. developed the friction stir welding (FSW) at the Welding Institute, U.K., and showed it to be substantially better than classical welding methods used for joining heterogeneous materials due to the absence of molten metal, elimination of radiation effect, and harmful emission of gases [2, 3]. FSW works on the principle of solid-state effect to plastically deform the workpiece material. The rubbing action between a non-consumable stirring tool, consisting of the shoulder and pin, and Astarita et al. reported that the rotational and traverse speeds of the tool, the geometry of the tool including its tilt angle, and the transverse force are the basic input variables of FSW which affect the properties of friction-welded joints [4]. Reasonable traverse and rotational speeds of the tool contribute to the proper flow of material after the deformation, around the tool, resulting in the formation of friction-welded joints.

Colligan et al. [5] applied the FSW technique to Al products in aerospace and automotive industries to fulfill the increased demand of light-weight components with concern for the environment. Kakimoto [6] used the FSW technique for welding AA2000 and AA7000 grade sheets, finding this

technique better than the traditional welding method. Cavaliere et al. [7] studied the microstructural and mechanical characteristics of AA 6082 joints made with FSW and examined the influence of various welding parameters. It has been reported that when the advancing speed is increased from 40 to 165 mm/min, there is a change in nugget mean grain size. However, when speed changes from slow speed to 115 mm/min, there is a significant increase in yield strength, but with further increase in advancing speed, yield strength decreases. The influence of tool traverse speed was studied for observing variation in microstructure and mechanical properties by Shen et al. [8] when FSW was done in the case of copper. It has been observed that with the increase in traverse speed, initially there was an increase in the grain size of the stirred region, but then it started decreasing. Furthermore, thermomechanically-affected region shrank and the boundary between these two regions became explicit, but there was no change in the heat-affected region. Ramkumar et al. [9] investigated the changes in the mechanical behavior of friction-stir welded AZ31 materials with respect to tool rotational speed and tool traverse speed ratio. It is confirmed that with the increase in the ratio, a slight decrease in ultimate and yield strength of the nugget region and transitional region was observed. Moreover, the size of the nugget region and incomplete root penetration were found to increase and decrease, respectively, when the rotational/traverse speed ratio was increased. Safi et al. [10] studied the warm FSW process for the dissimilar systems of AA7075 to Cu materials. It has been observed that by preheating the copper base material up to 175°C increases the mechanical behavior of the friction-welded joint by 100%.

To increase the weld strength in the FSW of the aluminium and Mg alloys, the FSW parameters such as tool rotational temperature, preheat treated workpiece speed, and traverse speed tool pin profiles were optimized using the Taguchi method [11]. The parameters were optimized for improving weld strength and interface [12]. The process parameters of the FSW process were optimized by Taguchi-response surface methodology (RSM) shows rapid improvement in the weld strength [13]. The Taguchi-based graph theory and matrix approach were applied to identify the optimal process parameter in FSW of AISI 304 stainless steel.

There is a lot of study on how Al/Mg alloys in the stir zone significantly affect the quality and performance of welding. In a small lap of time after its development, several research works have been carried out to enhance the mechanical properties of welding by controlling several weld parameters. Thus, the present research article's objective is to understand better how brass and aluminum alloy 6063 affect the joint's weld microstructure and mechanical properties. Finally, several strategies are highlighted to govern the FSW and the subsequent improvement of the weld joint properties, even though there are no study attempts to optimize the response parameters of friction stir welding of brass and AA6063 using the Taguchi L_{27} orthogonal array.

2. Materials and Methods for Experimentation

The objective of the experimental work was to optimize the FSW parameters for two dissimilar metals to improve the weld quality and hardness of welded joints.

The materials used in the present work were brass and commercial AA6063, an Al-Mg-Si-based alloy. AA6063 is typically produced with very smooth surfaces for anodizing. Both brass and AA6063 flat plates were cut into $145 \times 50 \times 6$ mm thickness. The cold plates were heated up to 300°C and 400°C for half an hour in the muffle furnace, with an extra holding time of 15 minutes. Heating times to the required temperature was varied from 0.5 to 3 hours, which was dependent on alloy type and load size. The preheated plates were welded with a number of different weld parameters. Experiments were conducted on a HURCO VM 10 (CNC universal vertical milling machine) to weld the plates with the Taguchi L_{27} experimental design. The plates were clamped in the machine firmly by placing the brass on the advancing side and AA6063 on the retreating side.

In FSW, the temperature was measured at various sections of the weld line using an infrared thermometer. However, direct measurement of temperature in the nugget zone is a cumbersome task, as combined rotation and translation of the tool cause intense plastic deformation in this zone [14, 15]. The temperature was recorded in full weld cycle for each sample 25 mm away, pointing at the rotating tool with an infrared thermometer. After heat treatment, the digital hardness test was performed with a full load set of 150 kgf and a dwell time equal to 10–15 s (make: HM-210 type A). The microscopic analysis was performed on different welded samples for studying the influence of various welding parameters on three zones, namely, nugget zone (NZ), heat-affected zone (HAZ), the thermomechanically-affected zone (TMAZ), and also on the base metal (BM). Table 1 presents the FSW process variables and their values at different levels and Figure 1(a) shows the FSW process image.

Three tool configurations, namely, square, triangular, and hexagonal, were used for fabricating the joints with a shoulder diameter of 16 mm and by considering the shoulder with and without concavity. The different process variables were tool traverse speed, rotational tool speed, pin profile of the tool, the temperature of the preheated workpiece, and the response variable of the friction-stir welded joint so produced, which is measured in terms of hardness and weld quality. Here, the microhardness value was measured perpendicular to the FSW joint at three locations along the nugget. At ambient temperature, the hardness values of AA6063 and brass were 70.2 and 76.7 HRB, respectively, whereas at 300°C, the hardness values were observed to be 73.7 and 80.8, respectively; however, at 400°C, the hardness values were found to be 75.6 and 84 HRB. Figure 1(a) shows the FSW and optical micrographs of polished AA6063 (Figure 1(b)) and brass (Figure 1(c)) obtained at 500x magnifications, and it can be noted that there is a change in microstructure with the increase in the temperature during heat treatment.

Table 1: FSW process variables and their values at various levels.

S. Nos.	Parameters	Notations	Units	Levels		
				Low	Medium	High
1	Tool rotational speed	N_{tool}	rpm	1200	1400	1600
2	Temperature of preheat treated workpiece	$T_{preheat}$	°C	36	300	400
3	Traverse speed	$S_{traverse}$	mm/min	16	24	32
4	Tool pin profile	P_{pin}	—	Hexagonal	Square	Triangular

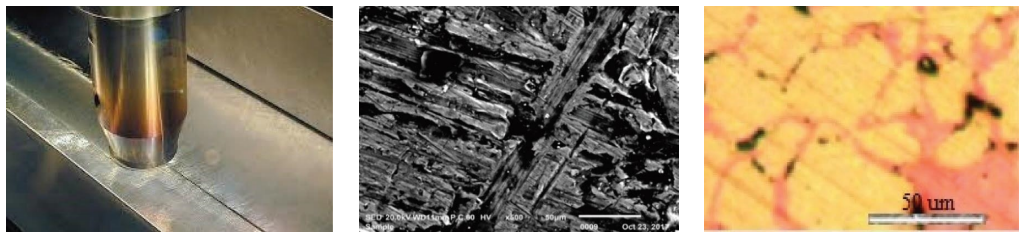

(a) (b) (c)

Figure 1: FSW image and microstructure of AA6063 and brass. (a) FSW image. (b) AA6063. (c) Brass.

3. Design of Experiments

The analysis of the obtained hardness data was performed to determine the influence of various process parameters. A "higher-the-better" performance criterion was considered to calculate the SNR of hardness with the following formula [16]:

$$SNR = -10\log\left(\frac{1}{k}\sum_{i=1}^{k}\frac{1}{(x_i)^2}\right), \quad (1)$$

where x_i, $i = 1, 2, 3, \ldots\ldots k$ are the response values under the trial conditions repeated $'k$ times.

In this case, the optimized result required is the higher hardness. Therefore, this criterion is chosen for finding the optimum process parameters. At each combination of the measured values, the experimental outcomes of the hardness were transformed into SNR. The use of SNR is recommended by Taguchi for measuring quality characteristics that deviate from desired values. The higher value of SNR implies better welding performance characteristics. Hence, the optimum level of input variables was taken as the level with a higher SNR. The most statistically relevant input variables were identified using analysis of variance (ANOVA). An optimized combination of these variables was predicted by considering both the ANOVA and SNR. The hardness results obtained at different combinations of process variables are presented in Table 2. A similar analysis for different processes has been carried out by various researchers [17–19].

4. Results and Discussion

The mean values obtained from the response variable, hardness, and the SNR for each variable at three levels were computed and shown in Tables 3 and 4, respectively. The influence of each factor viz. tool rotational speed (N_{tool}), temperature of preheating treated workpiece ($T_{preheat}$), traverse speed ($S_{traverse}$), and tool pin profile (P_{pin}) on the hardness of friction stir welded joint is depicted in Figure 2. The heat produced by frictional forces and material stirring will majorly affect hardness. The analysis of experimental data shows that grain refinement in the welded zone leads to higher hardness when compared to the base metal.

Figure 2(a) shows the variation in hardness with a change in tool rotational speed, which depicts the decrease in hardness when speed is increased. When tool rotational speed is low, less heat is generated, which results in lower recrystallization rates and ultimately a harder weld is achieved [17]. In addition to this, at low speeds, with less heat generation because of frictional forces and material stirring, small grain sizes lead to higher hardness [17]. It can be seen in Figure 2(b) that the preheating effect increases the hardness value upto 300°C and then decreases it. Such a phenomenon may be due to grain coarsening and work hardening due to the thermomechanical effect, recrystallization, and dynamic recovery [18]. Such a hardness trend is observed because of work hardening in the weld zone and not because of grain size [19].

Figure 2(c) exhibits a decrease in hardness value when the traverse speed is increased initially up to 24 m/min, then it starts rising. This may be attributed to the change in quantum and temperature of friction on the workpiece surface per unit of time with variation in traverse speed. The traverse speed of the tool determines the stirring of the rotating tool per mm of FSP , which affects the movement of material to the retreading side from the advancing side [20]. The hall-Petch relationship clearly states that the hardness has a reverse relevancy with grain size, which implies that if any parameter causes an effect on grain size, then hardness is bound to be affected [21]. Figure 2(d) clearly shows the effect of tool pin geometry on hardness values. The maximum hardness was observed with a hexagonal tool profile and the minimum with a triangular profile tool pin. In the hexagonal

Table 2: Taguchi L_{27} OA with measured hardness values and SNR.

Runs	N_{tool} (rpm)	$T_{preheat}$ (°C)	$S_{traverse}$ (mm/min)	P_{pin}	Hardness (HRB)	SNR
1	1200	36	16	Hexagonal	72.1	37.16
2	1200	36	16	Hexagonal	73.3	37.30
3	1200	36	16	Hexagonal	72.3	37.18
4	1200	300	24	Square	71.7	37.11
5	1200	300	24	Square	72.0	37.15
6	1200	300	24	Square	72.3	37.18
7	1200	400	32	Triangular	71.0	37.03
8	1200	400	32	Triangular	70.9	37.01
9	1200	400	32	Triangular	71.9	37.13
10	1400	36	24	Triangular	70.5	36.96
11	1400	36	24	Triangular	70.3	36.94
12	1400	36	24	Triangular	71.1	37.04
13	1400	300	32	Hexagonal	73.2	37.29
14	1400	300	32	Hexagonal	72.8	37.24
15	1400	300	32	Hexagonal	72.2	37.17
16	1400	400	16	Square	71.7	37.11
17	1400	400	16	Square	72.3	37.18
18	1400	400	16	Square	72.0	37.15
19	1600	36	32	Square	71.1	37.04
20	1600	36	32	Square	70.7	36.99
21	1600	36	32	Square	70.0	36.90
22	1600	300	16	Triangular	70.8	37.00
23	1600	300	16	Triangular	70.6	36.98
24	1600	300	16	Triangular	71.9	37.13
25	1600	400	24	Hexagonal	70.7	36.99
26	1600	400	24	Hexagonal	70.0	36.90
27	1600	400	24	Hexagonal	71.8	37.12

Table 3: Mean values and main effects of hardness (raw data).

Levels	N_{tool} (rpm)	$T_{preheat}$ (°C)	$S_{traverse}$ (mm/min)	P_{pin}
1	**71.94**	71.27	**71.89**	**72.04**
2	71.79	**71.94**	71.16	71.53
3	70.84	71.37	71.53	71.00
Delta	1.10	0.68	0.73	1.04
Rank	1	4	3	2

The bold values show the highest values.

Table 4: Mean values and main effects of hardness (SNR).

Levels	N_{tool} (rpm)	$T_{preheat}$ (°C)	$S_{traverse}$ (mm/min)	P_{pin}
1	**37.14**	37.06	**37.13**	**37.15**
2	37.12	**37.14**	37.04	37.09
3	37.01	37.07	37.09	37.02
Delta	0.13	0.08	0.09	0.13
Rank	1	4	3	2

The bold values shows the highest values.

tool profile, more redistribution of the second phase particles takes place in the matrix which causes a reduction in grain size and more magnesium silicide (Mg_2Si) particles distributed in the aluminum alloy [22]. A tool with a square pin profile has an intermediate hardness value as it experiences higher welding forces, which are the result of the eccentricity of the square pin profile and its pulsation effect. This increases tool wear, which asks for frequent replacement of tools and hence higher processing costs [23].

The S/N ratio values for the different input parameters have been depicted in Figure 3. A similar behavior of all the process parameters on hardness was observed. The hardness was found to be maximum at 1200 rpm tool rotational speed, 300°C temperature of preheat-treated workpiece, 16 mm/min traverse speed, and hexagonal tool pin profile.

An ANOVA was carried out to examine the significance of the input variables towards the hardness, and the residual data collected is depicted in Table 5. The model shows a reasonable value of *F*-probability, which recommends that all models are significant. It can be inferred that all input variables have significantly influenced hardness values. It has been noticed that rotational tool speed has the maximum effect on weldment quality with a 28.98% contribution, followed by the tool pin profile with a 22.30% contribution, and finally, travel speed and preheating effect with 11% and 10.95% contributions, respectively. The tool rotational speed parameter's contribution was also found to be most influential for the weld joint's performance [24]. The travel speed and preheating effect were found to have the least effect on the weld joint's performance.

4.1. Confirmation Experiments. The obtained optimal process variables were validated by conducting three confirmation experiments. The friction stir welding arrangement was set at $(N_{tool})_1$, $(T_{preheat})_2$, $(S_{traverse})_1$, and $(P_{pin})_1$, and the mean hardness value was measured as 73.80 HRB, which was within the confidence interval of the predicted optimal hardness for friction welded joints. *Optimal values of response characteristics (predicted means).*

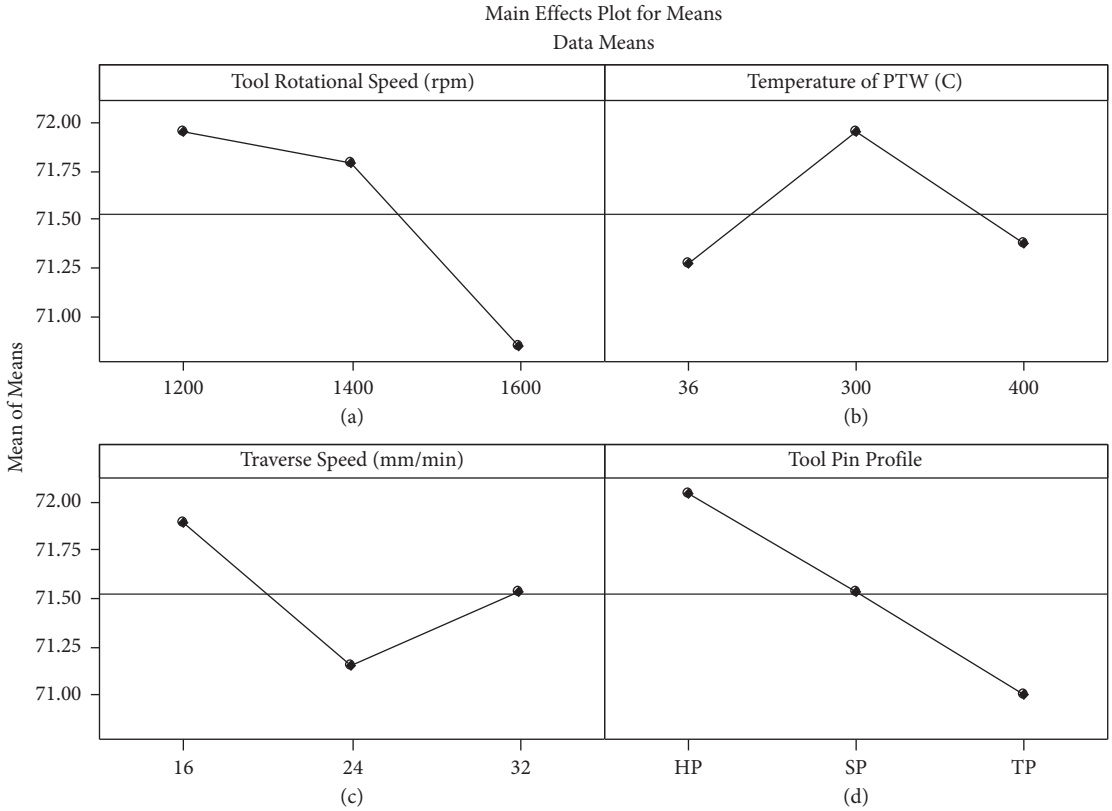

Figure 2: Variation of hardness with process parameters (raw data).

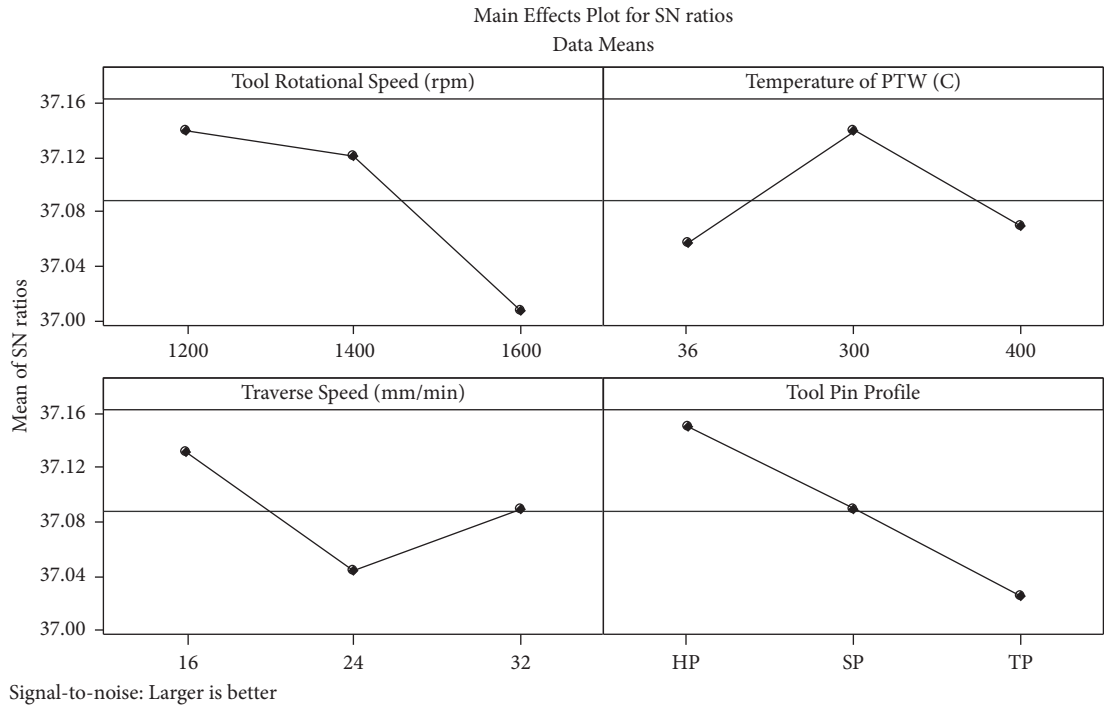

Figure 3: Variation of hardness with process parameters (SNR).

Table 5: Model significance of hardness using ANOVA.

Sources	DF	Seq SS	Adj SS	Adj MS	F	P	Percentage contribution
N_{tool} (rpm)	2	6.3785	6.3785	3.1893	9.74	0.001	28.98
$T_{preheat}$ (^{o}C)	2	2.4096	2.4096	1.2048	3.68	0.046	10.95
$S_{traverse}$ (mm/min)	2	2.4207	2.4207	1.2104	3.70	0.045	11.0
P_{pin}	2	4.9096	4.9096	2.4548	7.50	0.004	22.30
Error	18	5.8933	5.8933	0.3274			26.77
Total	26	22.0119					100

Note. DF, degrees of freedom; Seq SS, sequential sums of squares; Adj SS, adjusted sum of squares; Adj MS, adjusted mean square; F test of hypothesis, value of hypothesis (significant at 95% confidence level).

The optimal values of the predicted mean of the response parameter, i.e., hardness, can be obtained using the following equation and taking the data given in Table 4 into consideration:

$$\begin{aligned}\text{predicted mean hardness} &= (N_{\text{tool}})_1 + \left(T_{\text{preheat}}\right)_2 + (S_{\text{traverse}})_1 + \left(P_{\text{pin}}\right)_1 - 3 * \text{Y} \\ &= 73.22, \\ \text{percentage variation} &= +\frac{\{(73.80 - 73.22)\}}{73.80 * 100} = 0.79\,\%.\end{aligned} \tag{2}$$

4.2. Weld Morphology and Microstructure Analysis. The variation in temperature of the weld at various sections during welding was measured with the help of an infrared thermometer. The temperature was recorded in full weld cycle for each sample from a distance of 25 mm, pointing at the rotating tool. In every 25 mm, one reading of temperature was recorded. Figure 4(a) depicts the variation in temperature at various sections of the weld line. It can be observed that the temperature varies linearly with distance. The temperature in the multiple sections depends primarily on the coefficient of friction; a higher coefficient of friction leads to a higher temperature for a constant weld speed because the frictional force is also presumed to be proportional to the coefficient of friction [18, 25]. When the welding process is initiated, there is contact between the weld tool metal and weldpiece metal, which results in a regular and known value of the friction coefficient. When the welding process is further continued, softening of the weld piece surface is caused by the welding tool, which changes the value of the friction coefficient. The highest temperature attained among all the welded plates was 318°C when the rotational tool speed was 1600 rpm, the temperature value was 300°C, and the traverse speed of 16 mm/min with a triangular tool pin profile.

Figure 4(b) shows the variation of surface hardness at the weld line and various distances at various welding zones i.e., NZ, TMA), HAZ, and BM for all welded samples. The hardness is nearly constant in NZ, extending to 5 mm from each side of the weld joint. In TMAZ, which extends from 5 mm to 6 mm from the NZ, the hardness was observed to decrease, and the hardness achieved a minimum value in HAZ that extends from 15 mm to 20 mm from the TMAZ and then starts increasing. It has also been observed that the hardness of base metal was unaffected by FSW. Figures 5(a)–5(f) depict the optical micrographs and EDS-layered image of polished NZ of brass and AA6063.

Figure 5 shows the optimal microscope microstructure representation with different pin profiles and their effect on grain size at various values of tool rotational and travel speeds. While welding brass and AA6063, it is observed that the distribution between the brass and AA6063 shows the presence of boundary phenomena and a plastic combination of both metals in the stir zone [16]. Additionally, indicating that in this weld nugget zone of brass and AA6063, a lamellar alternating structure characteristic is observed towards the brass side [26]. However, in this weld nugget region, there is the presence of mixed structure characteristics of brass and AA6063 towards the aluminum side. The stirring action of the tool, generation of frictional heat, and heat conductivity characteristics of brass and AA6063 were responsible for the different structures of both sides of the weld nugget region. The centre of the nugget region had maximum hardness, because there was a formation of very fine recrystallized grains in this area. Three tool pin geometries, namely, hexagonal, square, and triangular, generated the pulsating stirring action, which led to a reduction in grain size and subsequently, homogenous redistribution of second phase particles in the entire matrix of the weld nugget region [27]. Continuous dynamic recrystallization had an overall impact on the hardness value in TMAZ and the nugget zone of AS. It is related to the fact that the change in strain rate due to the high-temperature deformation of pure aluminium depends on the combined effect of stress and temperature [28, 29]. This demonstrates that preheating leads to steady-state

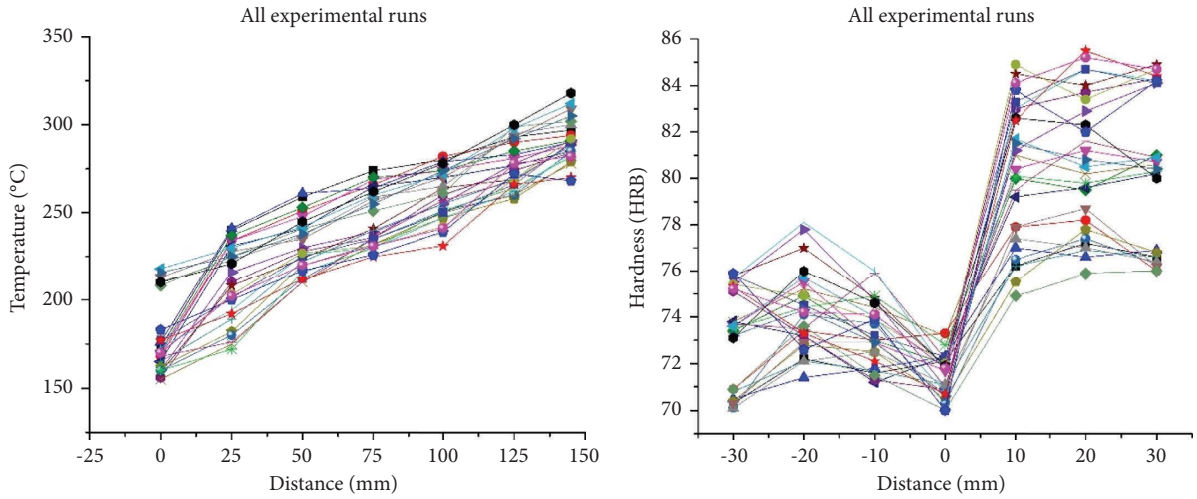

Figure 4: Variation in weld temperature and hardness at various sections and weld zones. (a) Weld temperature at different sections. (b) Weld joint hardness at different zones.

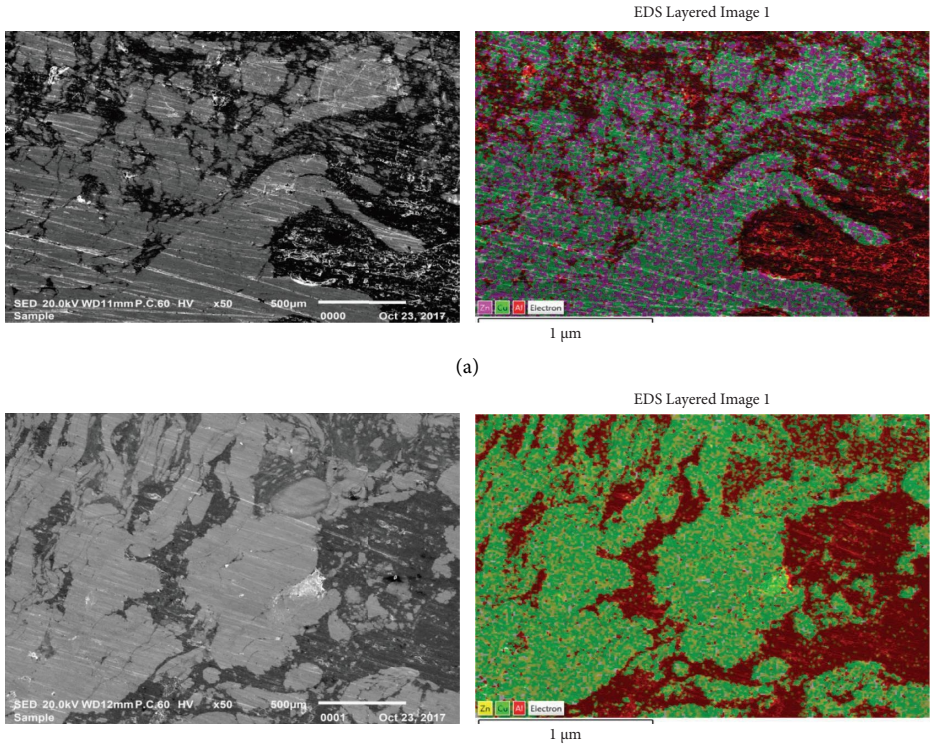

Figure 5: Continued.

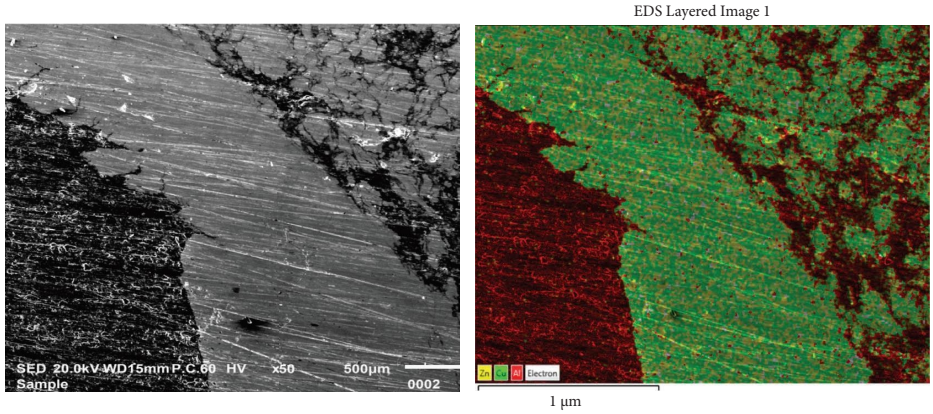

(c)

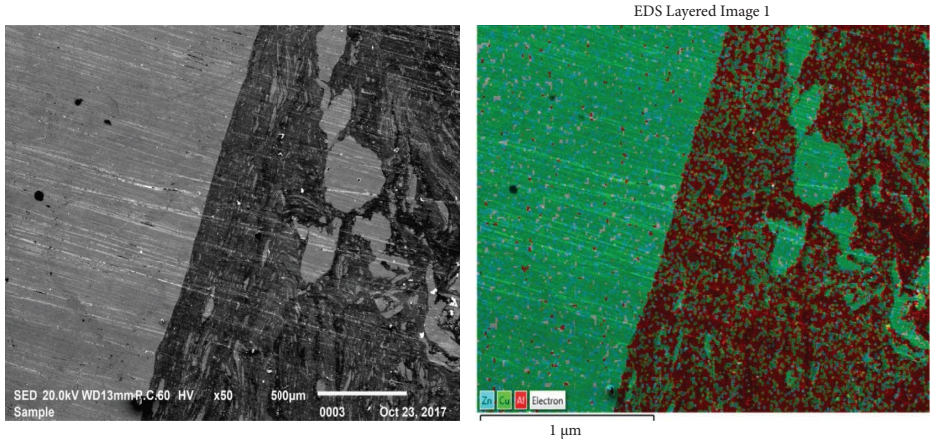

(d)

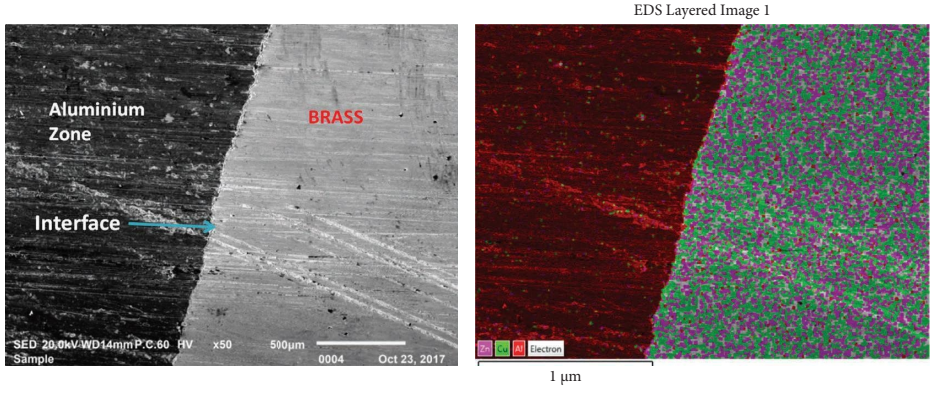

(e)

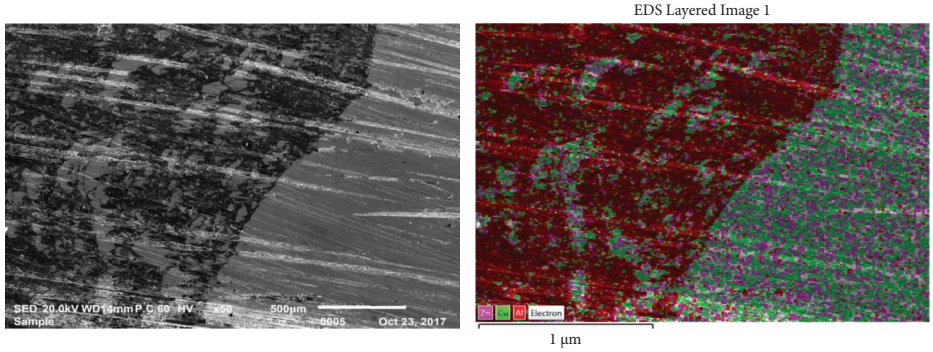

(f)

FIGURE 5: Optical microscope microstructure of the friction stir welded joints at different response parameters. (a) 1200 rpm, 36°C, 16 mm/min and HP. (b) 1200 rpm, 300°C, 24 mm/min, and SP. (c) 1200 rpm, 400°C, 32 mm/min, and TP. (d) 1400 rpm, 36°C, 24 mm/min, and TP. (e) 1400 rpm, 300°C, 32 mm/min, and HP. (f) 1400 rpm, 400°C, 16 mm/min, and SP.

deformation, which inculcates finer grain structure throughout the welded joint.

5. Conclusions

Friction stir-welded joints of brass and AA6063 have been prepared using the Taguchi L_{27} orthogonal array by varying different process parameters. Major conclusions of the current work have been listed below:

(1) The optimum levels of the rotational speed, traverse speed of the tool, preheated temperature, and tool pin profile were 1200 rpm, 16 mm/min, 300°C, and hexagonal, respectively.

(2) Tool rotation speed had a pronounced effect on microstructure, hardness, and the formation of defects in the welds, while traverse speed had comparatively less influence.

(3) Tool rotational speed was found to play a prominent role in increasing it and contributed 28.98% to the overall contribution.

(4) Optical microscopy identified three distinct zones, namely, the nugget zone (NZ), the thermomechanically affected zone (TMAZ), and the heat-affected zone (HAZ).

(5) The nugget zone had a maximum value of hardness (around 27% increase) due to the formation of very fine recrystallized grains.

(6) The maximum hardness was found with a hexagonal tool profile which was instrumental in providing fine grain structure and a higher distribution of Mg_2Si particles in aluminum alloy.

Data Availability

No data were used in this study.

Conflicts of Interest

The authors declare that there are no conflicts of interest.

References

[1] B. T. Gibson, D. H. Lammlein, T. J. Prater et al., "Friction stir welding: process, automation, and control," *Journal of Manufacturing Processes*, vol. 16, no. 1, pp. 56–73, 2014.

[2] W. M. Thomas, E. D. Nicholas, J. C. Needham, M. G. Murch, P. Temple-Smith, and C. J. Dawes, "Friction Stir Butt Welding, International Patent Application No. PCT/GB92/02203," 1991.

[3] R. I. Rodriguez, J. B. Jordon, P. G. Allison, T. Rushing, and L. Garcia, "Microstructure and mechanical properties of dissimilar friction stir welding of 6061-to-7050 aluminum alloys," *Materials & Design*, vol. 83, pp. 60–65, 2015.

[4] A. Astarita, A. Squillace, and L. Carrino, "Experimental study of the forces acting on the tool in the friction-stir welding of AA 2024 T3 sheets," *Journal of Materials Engineering and Performance*, vol. 23, no. 10, pp. 3754–3761, 2014.

[5] K. J. Colligan, P. J. Konkol, J. J. Fisher, J. James, and J. R. Pickens, "Friction stir welding demonstrated for combat vehicle construction," *Welding Journal*, vol. 82, pp. 34–40, 2003.

[6] H. Kakimoto, "Study on application of FSW to aircraft," *Journal - Japan Society for Technology of Plasticity*, vol. 46, p. 17, 2005.

[7] P. Cavaliere, A. Squillace, and F. Panella, "Effect of welding parameters on mechanical and microstructural properties of AA6082 joints produced by friction stir welding," *Journal of Materials Processing Technology*, vol. 200, no. 1-3, pp. 364–372, 2008.

[8] J. J. Shen, H. J. Liu, and F. Cui, "Effect of welding speed on microstructure and mechanical properties of friction stir welded copper," *Materials & Design*, vol. 31, no. 8, pp. 3937–3942, 2010.

[9] T. Ramkumar, A. Haiter Lenin, M. Selva kumar, M. Mohanraj, S. C. Ezhil Singh, and M. Muruganandam, "Influence of rotation speeds on microstructure and mechanical properties of welded joints of friction stir welded AA2014-T6/AA6061-T6 alloys," *Proceedings of the Institution of Mechanical Engineers-Part E: Journal of Process Mechanical Engineering*, vol. 9, 2022.

[10] S. V. Safi, H. Amirabadi, M. K. Besharati Givi, and S. M. Safi, "The effect of preheating on mechanical properties of friction stir welded dissimilar joints of pure copper and AA7075 aluminum alloy sheets," *The International Journal of Advanced Manufacturing Technology*, vol. 84, no. 9-12, pp. 2401–2411, 2016.

[11] S. Kamal, V. Parthiban, G. Puthilibai et al., "Investigation on tensile behaviour of different weld joints through Taguchi approach," *Advances in Materials Science and Engineering*, vol. 2022, Article ID 5258014, 9 pages, 2022.

[12] P. Sharma, S. Baskar, P. Joshi et al., "Optimization of process parameter on AA8052 friction stir welding using taguchi's method," *Advances in Materials Science and Engineering*, vol. 2022, Article ID 3048956, 8 pages, 2022.

[13] G. Sasikala, V. M. Jothiprakash, B. Pant et al., "Optimization of process parameters for friction stir welding of different aluminum alloys AA2618 to AA5086 by Taguchi method," *Advances in Materials Science and Engineering*, vol. 2022, Article ID 3808605, 9 pages, 2022.

[14] D. Kumar Patel, D. Goyal, and B. S. Pabla, "Optimization of parameters in cylindrical and surface grinding for improved surface finish," *Royal Society Open Science*, vol. 5, 2018.

[15] T. Goyal, R. S. Walia, and T. S. Sidhu, "Study of coating thickness of cold spray process using Taguchi method," *Materials and Manufacturing Processes*, vol. 27, no. 2, pp. 185–192, 2012.

[16] A. Heidarzadeh and T. Saeid, "Correlation between process parameters, grain size and hardness of friction-stir-welded Cu–Zn alloys," *Rare Metals*, vol. 37, no. 5, pp. 388–398, 2018.

[17] R. S. Mishra and Z. Y. Ma, "Friction stir welding and processing," *Materials Science and Engineering: R: Reports*, vol. 50, no. 1-2, pp. 1–78, 2005.

[18] D. K. Yaduwanshi, S. Bag, and S. Pal, "Effect of preheating in hybrid friction stir welding of aluminum alloy," *Journal of Materials Engineering and Performance*, vol. 23, no. 10, pp. 3794–3803, 2014.

[19] R. W. Fonda, K. E. Knipling, and J. F. Bingert, "Microstructural evolution ahead of the tool in aluminum friction stir welds," *Scripta Materialia*, vol. 58, no. 5, pp. 343–348, 2008.

[20] R. Sathiskumar, N. Murugan, I. Dinaharan, and S. J. Vijay, "Effect of traverse speed on microstructure and microhardness of Cu/B 4C surface composite produced by friction stir

processing," *Transactions of the Indian Institute of Metals*, vol. 66, no. 4, pp. 333–337, 2013.

[21] P. Lehto, H. Remes, T. Saukkonen, H. Hänninen, and J. Romanoff, "Influence of grain size distribution on the Hall-Petch relationship of welded structural steel," *Materials Science and Engineering A*, vol. 592, pp. 28–39, 2014.

[22] M. B. Bilgin and C. Meran, "The effect of tool rotational and traverse speed on friction stir weldability of AISI 430 ferritic stainless steels," *Materials & Design*, vol. 33, pp. 376–383, 2012.

[23] J. Marzbanrad, M. Akbari, P. Asadi, and S. Safaee, "Characterization of the influence of tool pin profile on microstructural and mechanical properties of friction stir welding," *Metallurgical and Materials Transactions B*, vol. 45, no. 5, pp. 1887–1894, 2014.

[24] K. Kamal Babu, K. Panneerselvam, P. Sathiya et al., "Parameter optimization of friction stir welding of cryorolled AA2219 alloy using artificial neural network modeling with genetic algorithm," *The International Journal of Advanced Manufacturing Technology*, vol. 94, no. 9-12, pp. 3117–3129, 2018.

[25] B. A. Kumar, M. M. Krishnan, A. F. Sahayaraj et al., "Characterization of the aluminium matrix composite reinforced with silicon nitride (AA6061/Si3N4) synthesized by the stir casting route," *Advances in Materials Science and Engineering*, vol. 2022, Article ID 8761865, 8 pages, 2022.

[26] M. Cabibbo, A. Forcellese, M. El Mehtedi, and M. Simoncini, "Double side friction stir welding of AA6082 sheets: microstructure and nanoindentation characterization," *Materials Science and Engineering A*, vol. 590, pp. 209–217, 2014.

[27] K. Elangovan and V. Balasubramanian, "Influences of tool pin profile and welding speed on the formation of friction stir processing zone in AA2219 aluminium alloy," *Journal of Materials Processing Technology*, vol. 200, no. 1-3, pp. 163–175, 2008.

[28] A. Bachmaier, M. Hafok, and R. Pippan, "Rate independent and rate dependent structural evolution during severe plastic deformation," *Materials Transactions*, vol. 51, no. 1, pp. 8–13, 2010.

[29] A. Nattappan, G. S. Priyadharshini, T. Satish Kumar, T. Velmurugan, M. Makeshkumar, and H L. allasi, "investigation into mechanical properties and sliding wear behavior of friction stir processed surface composite material," *Advances in Materials Science and Engineering*, vol. 2021, Article ID 8337568, 11 pages, 2021.